Conformational Analysis of Trimannoside and Bisected Trimannoside Using Aqueous Molecular Dynamics Simulations

Hyunmyung Kim, Youngjin Choi,† Jonghyun Lee, Karpjoo Jeong,* and Seunho Jung‡,*

*Department of Advanced Technology Fusion, Konkuk University, Seoul 143-701, Korea. *E-mail: jeongk@konkuk.ac.kr*
†Biochip Research Center, Hoseo University, Asan 336-795, Korea
*‡Department of Bioscience and Biotechnology & Bio/Molecular Informatics Center, Konkuk University, Seoul 143-701, Korea. *E-mail: shjung@konkuk.ac.kr*
Received September 26, 2009, Accepted October 5, 2009

The conformational properties of oligosaccharides are important to understand carbohydrate-protein interactions. A trimannoside, methyl 3,6-di-O-(α-D-Man)-α-D-Man (TRIMAN) is a basic unit of N-linked oligosaccharides. This TRIMAN moiety was further modified by GlcNAc (BISECT), which is important to biological activity of N-glycan. To characterize the trimannoside and its bisecting one we performed a molecular dynamics simulation in water. The resulting models show the conformational transition with two major and minor conformations. The major conformational transition results from the ω angle transition; another minor transition is due to the ψ angle transition of α (1 → 6) linkage. The introduction of bisecting GlcNAc on TRIMAN made the different population of the major and minor conformations of the TRIMAN moiety. Omega (ω) angle distribution is largely changed and the population of *gt* conformation is increased in BISECT oligosaccharide. The inter-residue hydrogen bonds and water bridges *via* bisecting GlcNAc residue make alterations on the local and overall conformation of TRIMAN moiety. These changes of conformational distribution for TRIMAN moiety can affect the overall conformation of N-glycan and the biological activity of glycoprotein.

Key Words: Bisecting GlcNAc, N-glycan, Molecular dynamics simulations

Introduction

The bisecting N-acetylglucosamine (GlcNAc) moiety is known to be a unique structure in asparagine-linked glycans (N-glycans). N-glycans with a bisecting GlcNAc lead to the inhibition of β(1 → 6) branch formation and therefore the biosynthesis of multi-antennary oligosaccharides was inhibited.[1] Reducing the number of β(1 → 6) branches, together with increasing bisected glycans in highly metastatic melanoma cell surface led to a suppression of lung metastasis of the melanoma cells.[2] Introduction of bisecting GlcNAc in N-glycan enhanced the activity of adenylyl cyclase III.[3] Furthermore, the presence of a bisecting GlcNAc affects the ligand properties of N-glycans.[4] These alterations of biological function are due to the conformational change of N-glycans. The addition of a bisecting GlcNAc caused a change of overall conformation of N-glycans.[5-6] The presence of a bisecting GlcNAc has a significant effect on conformation of the α1,6-linked mannose moiety.[1,4] Some groups investigated the conformation of bisected N-glycans using NMR and molecular modeling.[1,4-9] These groups investigated the conformation of a larger N-glycan than that of the TRIMAN moiety. The conformation around the α(1 → 6) linkage is influenced significantly by the addition/deletion of saccharides. It is necessary to scrutinize the local conformational behavior of bisecting GlcNAc with TRIMAN moiety in bisected N-glycan.

We describe a detailed study of the conformational distribution of methyl 3,6-di-O-(α-D-Man)-α-D-Man (TRIMAN) and its bisected one (BISECT) (Fig. 1) by molecular dynamics simulations. TRIMAN moiety is a part of the core structure of N-glycan and is one of the most commonly observed branch points in high mannose and hybrid types of N-glycan. The conformation of TRIMAN moiety has been investigated by NMR and molecular modeling approach.[10-13] In this paper, we investigated the effect of bisecting GlcNAc on the conformational change of TRIMAN moiety by MD simulations in water. The conformational characteristics of TRIMAN moiety in the presence of bisecting GlcNAc are important to understand N-glycan.

Computational Method

The starting models for simulations of TRIMAN and BISECT moieties were taken from the X-ray determined struc-

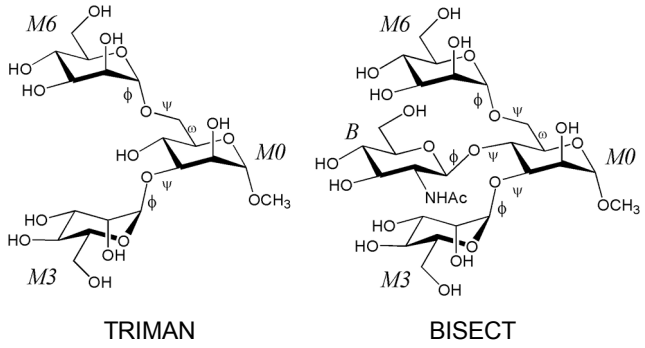

Figure 1. Structure of trimannoside and bisecting trimannoside. Glycosidic dihedral angles are labeled ϕ, ψ, and ω. The dihedral definitions were ϕ = O5(*i*)-C1(*i*)-O*n*(*i*-1)-C*n*(*i*-1), ψ = C1(*i*)-O*n*(*i*-1)-C*n*(*i*-1)-C(*n*-1)(*i*-1), ω = O6(*i*)-C6(*i*)-C5(*i*)-C4(*i*), where *i* indicates a given residue and *n* a ring position. The individual residues are denoted as letters, *M0*, *M3*, *M6*, and *B*, respectively.

ture of Vap2 in Protein Data Bank (PDB entry code 2DW and 2DW2).[14] Molecular dynamics simulations were carried out on the systems using the SANDER module of AMBER 10.0[15] with GLYCAM_06 force field.[16] The initial structures were built using the XLEAP module of AMBER. Each system was immersed in a 10 Å truncated octahedron periodic water box. The box of water molecules in system contains around 1100 TIP3P water molecules.[17] A 2 fs time step was used in all the simulations, and long-range electrostatic interactions were treated with the particle mesh Ewald (PME) procedure with a 10 Å nonbonded cutoff. Bond lengths involving hydrogen atoms were constrained using the SHAKE algorithm. Systems were minimized prior to the production run. The solvent molecules were first relaxed, while all atoms in oligosaccharides were restrained with the forces of 500 kcal $mol^{-1}Å^{-2}$. Then, the systems were continually relaxed. Finally, all restraints were lifted and whole system was relaxed with 1000 cycles of steepest descent followed by 1000 cycles of conjugate gradient minimization. After relaxation, 300 ps MD simulations were carried out at constant volume, with 10 kcal mol^{-1} $Å^{-2}$ restraints on solute. Then 80 ns of NPT MD simulations were carried out on systems at constant pressure (1 atm). All simulations were performed at 300 K except the equilibrium MD run. The PTRAJ module of AMBER was used to analyze the results. The RMSD values were calculated only for heavy atoms of oligosaccharides after superimposing conformations on the *M0* residue of oligosaccharides. The hydrogen bonds were defined as hydrogen acceptor-donor atom distances of less than 3.5 Å and acceptor-H-donor angles of more than 120^{o}. The hydrogen bonds of water bridges were also investigated with the same distance and angle cutoff values. The conformations were extracted from clusters of each oligosaccharide by PTRAJ module with means algorithms implemented in AMBER.[18]

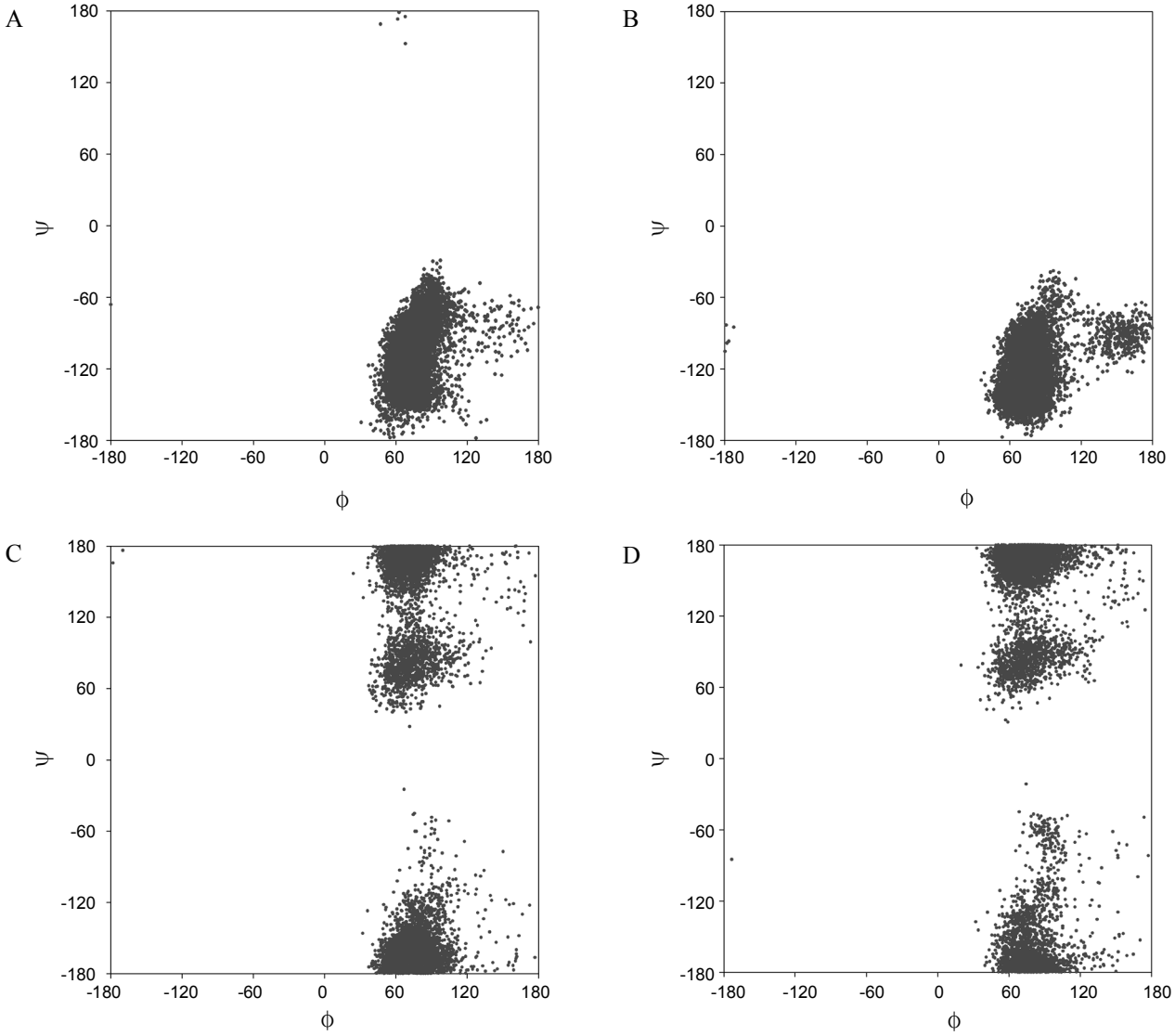

Figure 2. Scatter plots of the ϕ and ψ trajectories from MD simulations. (A) α-Man-(1 → 3)-Man linkage of trimmanoside (TRIMAN); (B) α -Man-(1 → 3)-Man linkage of bisecting trimmanoside (BISECT); (C) α-Man-(1 → 6)-Man linkage of TRIMAN; (D) α-Man-(1 → 6)- Man linkage of BISECT.

Results and Discussion

The simulations were performed for a total of 80 ns at a constant temperature of 300 K. Figure 2A shows the exploration of α(1 → 3) linkage of TRIMAN during the simulations. The α(1 → 3) linkage was restricted in conformational space to a single region, as described previously.[7,12,19-20] Although there are additional minor conformational spaces,[11] we considered a single conformational space in this study. The average conformation (76 ± 15°, −107 ± 25°) is similar to that observed in the X-ray crystal structure (72 ± 9°, −120 ± 17°).[21] In the case of the bisected one (BISECT), the average conformation (77 ± 20°, −123 ± 22°) is similar to the experimentally observed one[21] and shows a single conformational space (Fig. 2B). These results indicate that bisecting GlcNAc shows minimal effect on the conformation of α(1 → 3) linkage of TRIMAN moiety. In the case of α(1 → 6) linkage, distinct conformations were observed in the MD simulations. Though constant φ values (74 ± 16° in TRIMAN, 77 ± 17° in BISECT) were observed (Fig. 2C, 2D), both ψ and ω angles are distributed in two separated conformations in both oligosaccharides.

Statistic analysis of the X-ray data and NMR data indicated the presence of both *gg* and *gt* conformations at the α(1 → 6) linkage,[12,21] where the *gg* conformation corresponds to ω = ± 180° and *gt* to ω = +60°. Analysis of the residual dipolar couplings suggested that both the *gg* and *gt* conformation are possible at the α(1 → 6) linkage of TRIMAN with almost equal populations.[12] For the α(1 → 6)-mannobioside, the *gg*/*gt* ratio obtained by scalar coupling analysis is *ca*. 1 : 1.[22] Figure 3 shows the ω angle transition of three oligosaccharides in 80 ns MD simulations. The ω angle transitions between *gg* and *gt* conformation are observed in all three oligosaccharides. At the α(1 → 6)-mannobioside the transition occurs in 14 ns and the *gg*/*gt* ratio of 80 ns MD simulation is 1.01, which is in good agreement with experimental data.[22] However, the *gt* conformations of TRIMAN and BISECT are maintained up to 21 and 44 ns and the *gg*/*gt* ratios of 80 ns MD simulation are 0.23 and 0.34, respectively. The calculations of TRIMAN appear to overestimate the population of the *gt* conformation of experimental data.[12] This phenomenon is observed in other long MD simulation of TRIMAN with CHARMM force field where *gg* conformation exchanges to *gt* conformation after 8.5 ns MD simulation and there is no conformational exchange following 41.5 ns.[12] Molecular modeling of (1 → 6) linkage of saccharide has been difficult to generate the correct rotamer populations for the ω angle because of weaknesses in the force fields and omission of the solvent effects.[23] However, MD simulation of α(1 → 6)-mannobioside in this study correctly predicted the rotamer population. In the case of TRIMAN and previously reported larger N-glycan, there are disagreements of experimental rotamer populations.[12] This may be due mainly to the solvent effect of the simulation. Sampling of ω rotamers of α(1 → 6) linkage conformation may be improved with a refined model for water.

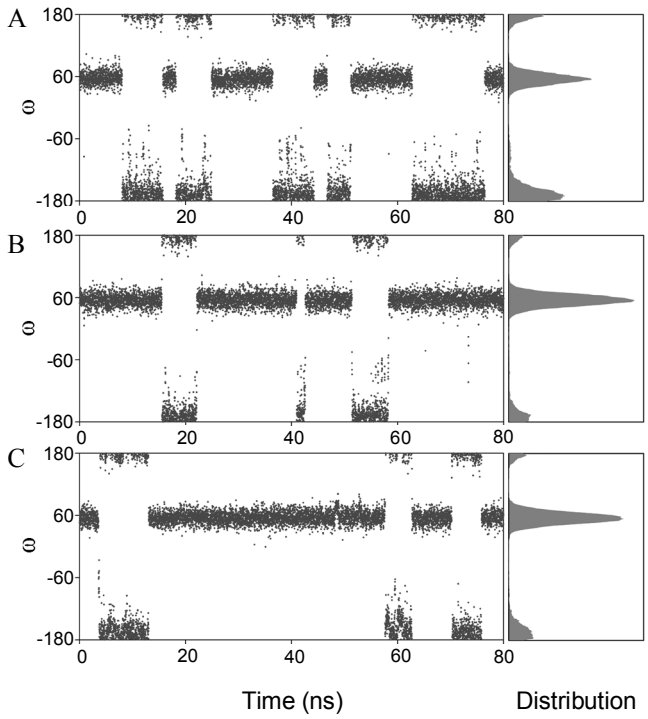

Figure 3. Conformational transition and distribution of ω dihedral angles for (A) α(1 → 6)-mannobioside, (B) TRIMAN, and (C) BISECT oligosaccharides as a function of elapsed time in the MD simulations.

The major conformational change of oligosaccharides is due to the transition of ω angle of α(1 → 6) linkage of oligosaccharides. Figure 4 shows the dynamics of two major conformations (*gg* and *gt* rotamers) of each oligosaccharide. The overall flexibility of the oligosaccharide and the particular flexibility of the α(1 → 6) linkage are clearly observed. The additional minor flexibility mainly came from the transition of ψ angle of α(1 → 6) linkage. Figure 2C and 2D shows the exploration of φ and ψ angles of α(1 → 6) linkage during the MD simulations of oligosaccharides. There are two clear populations in conformational space in both oligosaccharides. The average ψ angles of each population of TRIMAN are *ca*. 82 ± 16° and 188 ± 21° and those of BISECT are 84 ± 15° and 178 ± 26°. These angles are similar to those of the X-ray

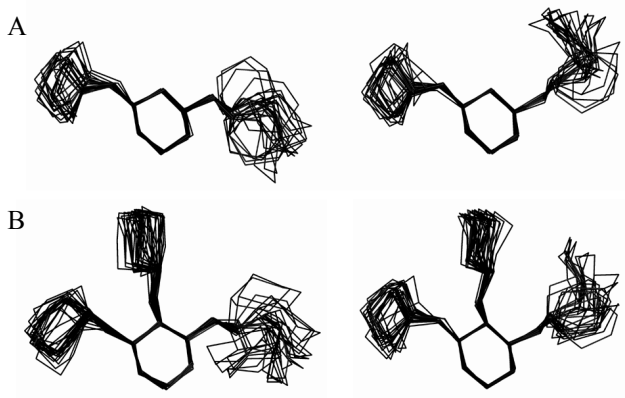

Figure 4. The flexible conformations of (A) TRIMAN and (B) BISECT oligosaccharides. The conformations on the left and right are *gg* and *gt* rotamers of each oligosaccharide, respectively. The ring and glycosidic linage atoms were drawn in this diagram for clarity. The conformations were superimposed on the *M0* residues of oligosaccharide.

crystal structure (94 ± 18° and *ca.* 180°)[21] and previously reported results.[12,24] The transition of ψ angle of α(1 → 6) linkages remained predominantly near 180° and transiently populated another state. At the *gt* conformation of the linkage the ψ angle conformation near 80° is 8.7 and 10.1% in TRIMAN and BISECT, respectively. However, at the *gg* conformation of the linkage, the ψ angle conformation near 80° is increased up to 34.3 and 18.7% in each oligosaccharide. These results can show why the *gt* conformation with near 90° ψ angle is not observed in the X-ray crystal structure.[21]

Although there is some deviated distribution of ϕ-ψ conformational map in BISECT comparing with TRIMAN, no clear difference between oligosaccharides is observed (Fig. 2). This indicates that there is no steric hindrance by introducing bisecting GlcNAc on TRIMAN oligosaccharide. The deviation may come from the additional interaction of Man residues with bisecting GlcNAc (B residue). This will be discussed with the inter-residue hydrogen bonds and water bridges. The introduction of bisecting GlcNAc on TRIMAN mainly affects the α(1 → 6) linked Man moiety (*M6* residue). The overall RMSD of *M3* residues of TRIMAN and BISECT is similar and is in the range of standard deviation. However, the RMSD of *M6* residue is greatly reduced in both *gg* and *gt* conformations of BISECT than that of TRIMAN oligosaccharide. RMSD values of *M6* residue of *gg* and *gt* conformations are 0.45 ± 0.15 and 0.35 ± 0.20 in TRIMAN and 0.28 ± 0.15 and 0.23 ± 0.13 in BISECT, respectively.

Figure 5 shows the exploration of β(1 → 4) linkage of methyl 4-O-α-D-Man-β-D-GlucNAc disaccharide and BISECT during the simulations. Bisecting GlcNAc has rather limited flexibility and its relative orientation with respect to the *M0* residue remains very nearly the same.[9] The β(1 → 4) linkage of disaccharide was restricted in conformational space to a single region and the average conformation is *ca.* (−81 ± 13°, 108 ± 17°). However, the conformation of linkage β(1 → 4) linkage of BISECT clearly shows two region and the average conformations are *ca.* (−115 ± 12°, 78 ± 11°; *B1*) and (−69 ± 12°, 126 ± 8°; *B2*), respectively (Fig. 5B). B2 conformation of β(1 → 4) linkage in BISECT is similar to that observed in the NMR restrained MD simulations of bisected biantenanary octasaccharide (*ca.* −56°, 126°).[7] The bisecting GlcNAc (residue *B*) interacts with adjacent residues *via* hydrogen bonding. Table 1 shows the hydrogen bonds between inter-residues of BISECT. The bisecting GlcNAc residue mainly interacts with *M3* residues at B1 conformation and with *M6* residues at B2 conformation. These results indicate that the GlcNAc moiety interacts with adjacent sugar residues and can affect the conformation of TRIMAN moiety by changing its linkage conformation.

Although the intramolecular hydrogen bonds are important, the water bridges between the residues are also a major factor to determine the molecular conformations of oligosaccharides.[13,25] The water bridges between residues were observed in both *gg* and *gt* conformations during the simulations. We analyzed individual conformations of oligosaccharides and only considered single and dimer water bridges whose occupancies were more than 10% in the period of each *gg* and *gt* rotamers of oligosaccharides. At the TRIMAN structure, results for water bridges between residues are similar to the results of Almond *et al.*[13] Dimer water bridges between O2 of *M0* and O4 of *M3* were observed more than 20%. Water bridges between *M0* and *M6* residues are largely different according to *gg* and *gt* conformation of TRIMAN. Single and dimer water bridges between O4 of *M0* and O6 of *M6* were

Table 1. Hydrogen bonds between the residues of BISECT oligosaccharide.

β(1 → 4) linkage Conformations	Residues / Group[a]		Occupancy (%)
	GlcNAc (*B*)	Man (*M3*, *M6*)	
B1	*B* / O6	*M3* / H-O2	35.26
	B / H-O6	*M3* / O2	12.13
B2	*B* / H-N2	*M6* / O6	36.01

[a]The atom pairs were only listed above 10% occupancies.

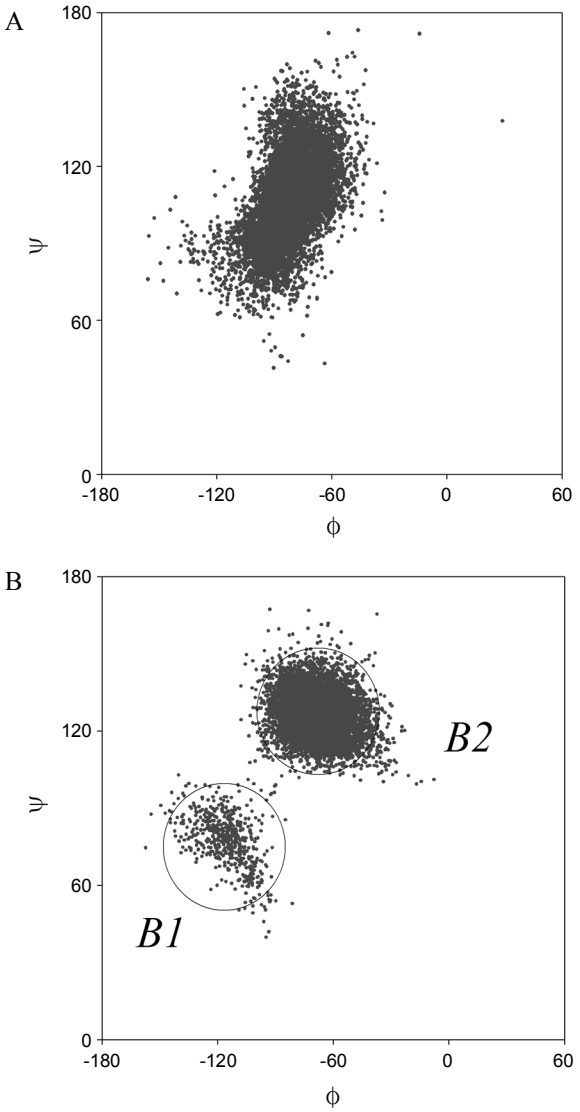

Figure 5. Scatter plots of the ϕ and ψ trajectories from MD simulations for the β-GlcNAc-(1 → 4)-Man linkage of (A) methyl 4-O-α-D-Man-β-D-GlcNAc and (B) BISECT oligosaccharides. Two conformations of BISECT (*B1* and *B2*) are indicated with open circles.

Table 2. Water bridges between the residues of BISECT oligosaccharides.

Conformation	Inter-residues	Related Atoms of each inter-residues[a]
gg	*B--M3*	**O6--O3**, O3--O2, **ON2--O2**, **ON2--O6**, ON2--O5
	B--M6	N2--O5, N2--O2
	B--M0	**O6--O2**
gt	*B--M3*	**O6--O3**, O3--O2, **ON2--O2**, ON2--O6
	B--M6	**N2--O6**, **O6--O4**, **O6--O3**, **O4--O4**, O3--O6
	B--M0	**O6--O2**

[a]The atom pairs were only listed above 10% occupancies and the bold character atom pairs are above 30% occupancies with single and dimer water bridges.

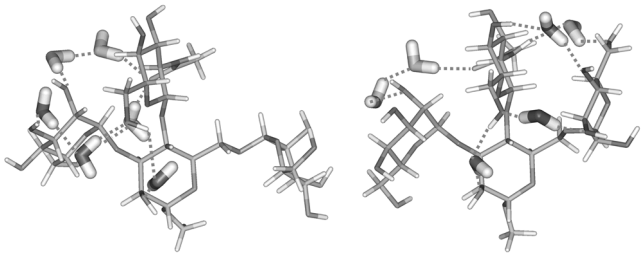

Figure 6. Representative conformations of *gg* (left) and *gt* (right) rotamers of BISECT with water bridges.

observed in *gg* conformation. However, in the case of *gt* conformation, multiple water bridges were observed with high occupancies (O4-*M0*--O6-*M6*, O4-*M0*--O4-*M6* and O2-*M0*--O4-*M6*).[13] The dimer water bridges were also observed between *M3* and *M6* residue with 10% occupancy in *gt* conformation of TRIMAN. This can be one of the reasons why *gt* conformation is overestimated in TRIMAN in spite of the correct estimation of *gg*/*gt* population in mannobioside.

In the case of BISECT oligosaccharides, the water bridges between residues are more complicated than in TRIMAN and mainly observed *via* bisecting GlcNAc (*B*) residue (Fig. 6). The dimer water bridges between *M0* and *M3* residues are slightly reduced compared to those in TRIMAN. In the *gg* conformation, new single and dimer water bridges were observed between O5 of *M0* and O4 of *M6* and between O2-*M0* and O6-*M6*, respectively. In the *gt* conformation, only dimer water bridges between O2-*M0* and O3-*M6* remained because of the loss of O4 hydroxyl group and the addition of *B* residue. Other additional water bridges were formed *via B* residue. In addition to inter-residue hydrogen bonds with *B* residue (Table 1), there are the large numbers of water bridges *via B* residue in BISECT (Table 2). Water bridges between *B* and *M6* residues of *gt* conformation show the highest occupancy. This can explain why *gt* conformation of BISECT was observed in a longer simulation time than that of TRIMAN (Fig. 3).

As mentioned above, M6 residue is more flexible than M3 residue in both oligosacchairdes (Fig. 4). We also investigated the local flexibility of $\alpha(1 \rightarrow 6)$ and $\alpha(1 \rightarrow 3)$ linked disaccharide moieties (*M0-M6* and *M0-M3*) of oligosaccharides. After the introduction of bisecting GlcNAc, the conformational fluctuation of disaccharide moiety is observed. Local flexibility is similar according to *gg*/*gt* conformations in TRIMAN, but clearly dependent on *gg*/*gt* conformations in BISECT. RMSD values of *M0-M6* are 1.00 ± 0.47 and 1.09 ± 0.30 and those of *M0-M3* are 0.61 ± 0.26 and 0.60 ± 0.22 in *gg* and *gt* conformations of TRIMAN, respectively. Without bisecting residue, there is no deviation of RMSD of *M0-M6* and *M0-M3* moieties according to *gg*/*gt* conformation. After introducing bisecting GlcNAc to TRIMAN moiety, RMSD of *M0-M6* and *M0-M3* moieties are increased and dependent on the *gg*/*gt* conformation of BISECT. A bisecting GlcNAc restrains the fluctuation of *M3-M0* fragment only when a GlcNAc is $\beta(1 \rightarrow 2)$ linked to *M3* residue.[9] In *gg* conformation the difference is observed in *M0-M3* moiety and the value is increased to 0.83 ± 0.14. In *gt* conformation the difference is observed in *M0-M6* moiety and the value is increased to 1.73 ± 0.43. Other RMSD values are slightly increased compared with those of TRIMAN in the range of standard deviation. These are due to the additional different interactions *via B* residues, which results in the somewhat deviated distribution of ϕ-ψ conformational map between oligosaccharides. The main interactions of *B* residue with *M3* and *M6* residues by inter-residue hydrogen bonds and water bridges are differently observed in *gg* and *gt* conformation of BISECT, respectively (Table 1 and 2).

Conclusion

We investigated the conformational characteristics of trimannoside and bisecting trimannoside parts of N-glycans by molecular dynamics simulations. Molecular dynamics simulations of these oligosaccharides in water box give us information about the effect of bisecting GlcNAc moiety on core trimannoside structure of N-glycans. GlcNAc moiety (*B* residue) breaks the inter-residue interactions of the TRIMAN moiety. According to *gg* and *gt* conformation, inter-residue hydrogen bonds and water bridges are observed in a different manner. In *gt* conformation, the largest numbers of water bridges between *B* and *M6* residues are observed in the BISECT oligosaccharide, which gives longer maintenance of this conformation than in the TRIMAN oligosaccharide. These additional inter-residue interactions make changes in the local flexibility of $\alpha(1 \rightarrow 6)$ and $\alpha(1 \rightarrow 3)$ linked disaccharide moieties according to *gg*/*gt* rotamer conformations. These results show that the introduction of bisecting GlcNAc on N-glycans can trigger different conformational preferences of local structure (TRIMAN moiety), which lead to the alteration of overall conformation in N-glycans.

Acknowledgments. This work was supported by a grant of Basic Science Research Program through the National Research Foundation of Korea (NRF) funded by the Ministry of Education, Science and Technology (2009-0059986) and partly by Priority Research Centers Program through NRF funded by the Ministry of Education, Science and Technology (2009-0093824).

References

1. Taniguchi, N.; Yoshimura, M.; Miyoshi, E.; Ihara, Y.; Nishikawa, A.; Fujii, S. *Glycobiology* **1996**, *6*, 691.
2. Yoshimura, M.; Nishikawa, A.; Ihara, Y.; Taniguchi, S.; Taniguchi, N. *Proc. Natl. Acad. Sci. USA* **1995**, *92*, 8754.
3. Li, W.; Takahashi, M.; Shibukawa, Y.; Yokoe, S.; Gu, J.; Miyoshi, E.; Honke, K.; Ikeda, Y.; Taniguchi, N. *Glycobiology* **2007**, *17*, 655.
4. André, S.; Unverzagt, C.; Kojima, S.; Frank, M.; Seifert, J.; Fink, C.; Kayser, K.; von der Lieth, C.-W.; Gabius, H.-J. *Eur. J. Biochem.* **2004**, *271*, 118.
5. Brisson, J. R.; Carver, J. P. *Biochemistry* **1983**, *22*, 3671.
6. Brisson, J. R.; Carver, J. P. *Biochemistry* **1983**, *22*, 3680.
7. Rutherford, T. J.; Homans, S. W. *Biochemistry* **1994**, *33*, 9606.
8. Balaji, P. V.; Qasba, P. K.; Rao, V. S. R. *Int. J. Biol. Macromol.* **1996**, *18*, 101.
9. Qasba, P. K.; Balaji, P. V.; Rao, V. S. R. *J. Mol. Struct.* **1997**, *395-396*, 333.
10. Brisson, J. R.; Carver, J. P. *Biochemistry* **1983**, *22*, 1362.
11. Sayers, E. W.; Prestegard, J. H. *Biophys. J.* **2000**, *79*, 3313.
12. Almond A.; Duus J. Ø. *J. Biomol. NMR* **2001**, *20*, 351.
13. Almond, A. *Carbohydr. Res.* **2005**, *340*, 907.
14. Igarashi, T.; Araki, S.; Mori, H.; Takeda, S. *FEBS Lett.* **2007**, *581*, 2416.
15. Case, D. A.; Darden, T. A.; Cheatham, T. E. *et al.* AMBER 10, University of California, San Francisco, 2008.
16. Kirschner, K. N.; Yongye, A. B.; Tschampel, S. M.; González-Outeiriño, J.; Daniels, C. R.; Foley, B. L.; Woods, R. J. *J. Comput. Chem.* **2008**, *29*, 622.
17. Jorgensen, W. L.; Chandrasekhar, J.; Madura, J. D.; Imprey, R. W.; Klein, M. L. *J. Chem. Phys.* **1983**, *79*, 926.
18. Shao, J.; Tanner, S. W.; Thompson, N.; Cheatham, T. E. 3rd. *J. Chem. Theory Comput.* **2007**, *3*, 2312.
19. Dowd, M. K.; French, A. D. *J. Carbohyd. Chem.* **1995**, *14*, 589.
20. Homans, S. W.; Pastore, A.; Dwek, R. A.; Rademacher, T. W. *Biochemistry* **1987**, *26*, 6649.
21. Wormald, M. R.; Petrescu, A. J.; Pao, Y.-L.; Glithero, A.; Elliott, T.; Dwek, R. A. *Chem. Rev.* **2002**, *102*, 371.
22. Spronk, B. A.; Rivera-Sagredo, A.; Kamerling, J. P.; Vliegenthart, J. F. G. *Carbohydr. Res.* **1995**, *273*, 11.
23. Kirschner, K. N.; Woods, R. J. *Proc. Natl. Acad. Sci. USA* **2001**, *98*, 10541.
24. Woods, R. J.; Pathiaseril, A.; Wormald, C. J.; Dwek, R. A. *Eur. J. Biochem.* **1998**, *258*, 372.
25. Corzana, F.; Motawia, M. S.; Penhoat, C. H.; Berg, F.; Blennow, A.; Perez, S.; Engelsen, S. B. *J. Am. Chem. Soc.* **2004**, *126*, 13144.